Title

Complex I dysfunction underlies the glycolytic switch in pulmonary hypertensive smooth muscle cells.

Authors

Rafikov, Ruslan
Sun, Xutong
Rafikova, Olga
et al.

Publication Date

2015-12-01

DOI

10.1016/j.redox.2015.07.016

Peer reviewed

Redox Biology 6 (2015) 278–286

Contents lists available at ScienceDirect

Redox Biology

journal homepage: www.elsevier.com/locate/redox

Complex I dysfunction underlies the glycolytic switch in pulmonary hypertensive smooth muscle cells

Ruslan Rafikov [a,b,*], Xutong Sun [a,b], Olga Rafikova [a,b], Mary Louise Meadows [c], Ankit A. Desai [b], Zain Khalpey [d], Jason X.-J. Yuan [a,b], Jeffrey R. Fineman [e,f], Stephen M. Black [a,b,*]

[a] Division of Translational and Regenerative Medicine, The University of Arizona, Tucson, AZ, USA
[b] Department of Medicine, The University of Arizona, Tucson, AZ, USA
[c] Vascular Biology Center, Georgia Regents University, Augusta, GA, USA
[d] Department of Surgery, The University of Arizona, Tucson, AZ, USA
[e] Department of Pediatrics and the University of California San Francisco, San Francisco, CA, USA
[f] Cardiovascular Research Institute, University of California San Francisco, San Francisco, CA, USA

ARTICLE INFO

Article history:
Received 23 June 2015
Received in revised form
21 July 2015
Accepted 28 July 2015
Available online 31 July 2015

Keywords:
Warburg effect
Electron transport chain
Pulmonary hypertension
Mitochondria

ABSTRACT

ATP is essential for cellular function and is usually produced through oxidative phosphorylation. However, mitochondrial dysfunction is now being recognized as an important contributing factor in the development cardiovascular diseases, such as pulmonary hypertension (PH). In PH there is a metabolic change from oxidative phosphorylation to mainly glycolysis for energy production. However, the mechanisms underlying this glycolytic switch are only poorly understood. In particular the role of the respiratory Complexes in the mitochondrial dysfunction associated with PH is unresolved and was the focus of our investigations. We report that smooth muscle cells isolated from the pulmonary vessels of rats with PH (PH-PASMC), induced by a single injection of monocrotaline, have attenuated mitochondrial function and enhanced glycolysis. Further, utilizing a novel live cell assay, we were able to demonstrate that the mitochondrial dysfunction in PH-PASMC correlates with deficiencies in the activities of Complexes I–III. Further, we observed that there was an increase in mitochondrial reactive oxygen species generation and mitochondrial membrane potential in the PASMC isolated from rats with PH. We further found that the defect in Complex I activity was due to a loss of Complex I assembly, although the assembly of Complexes II and III were both maintained. Thus, we conclude that loss of Complex I assembly may be involved in the switch of energy metabolism in smooth muscle cells to glycolysis and that maintaining Complex I activity may be a potential therapeutic target for the treatment of PH.

1. Introduction

Mitochondria convert nutrients into ATP using a highly effective energy-transformation process. ATP production by mitochondria involves the oxidation of glucose that generates 36 mol of ATP per 1 mol of glucose. The cytosolic production of energy called – glycolysis is far less efficient and produces only two ATP molecules per glucose. However, glycolysis is still required for mitochondrial ATP production, because it supplies the pyruvate molecules necessary for mitochondrial activity. Therefore, under physiologic conditions, cells use both mitochondrial oxidative phosphorylation and glycolysis for energy generation. However, it is becoming increasingly evident that under certain disease conditions there is damage to the mitochondrion that limits its ability to generate ATP via oxidative phosphorylation. Under these conditions of mitochondrial dysfunction, cells switch from oxidative phosphorylation to an aerobic glycolytic production of ATP, the so-called Warburg effect.

The mitochondrial electron transfer chain consists of five distinct Complexes. Electrons enter the respiratory chain at Complex I from NADH, or Complex II as it catabolizes succinate. Both Complexes transfer electrons to Coenzyme Q, which then shuttles the electrons to Complex III. Cytochrome c further transfers electron to Complex IV, which combines them with oxygen to produce water. All four Complexes use energy from the electron flow to pump protons from the mitochondrial matrix into the intermembrane space. The proton gradient generated in this process adds about 40% of its energy to the synthesis of ATP via Complex V. Thus, together, Complexes I–IV, CoQ and cytochrome c form the electron

* Corresponding authors at: Division of Translational and Regenerative Medicine, Department of Medicine, The University of Arizona, Tucson, AZ 85724, USA.
E-mail addresses: ruslanrafikov@deptofmed.arizona.edu (R. Rafikov), steveblack@email.arizona.edu (S.M. Black).

http://dx.doi.org/10.1016/j.redox.2015.07.016
2213-2317/

transport chain and with Complex V, ATP synthase, they form the mitochondrial respiratory chain. Under physiologic conditions, vascular smooth muscle cells (SMC) exist in a differentiated, contractile state. However, SMC are susceptible to phenotype modulation [1]. During this process, SMC undergo a transition from their normal contractile, differentiated phenotype to one that exhibits a synthetic proliferative, dedifferentiated phenotype [2,3]. This phenotype modulation contributes to the pathogenesis of a number of cardiovascular disorders, including pulmonary hypertension (PH) [4,5]. Recent work both from our lab, and others, has identified impaired mitochondrial function in PASMC [6,7] and PAEC [8–11] in PH that results in a survival advantage [11]. This survival advantage is thought to be due to the cells switching from oxidative phosphorylation to glycolysis, in order to generate cellular ATP [12]. However, the underlying mechanisms responsible for this glycolytic switch are still unresolved. In particular, it is unclear where, within the mitochondrial respiratory chain, do the derangements lie.

Thus, the focus of this study was to determine if there are defects in the activities of the electron transport system in PASMC isolated from rats with PH. Our data indicate the mitochondrial dysfunction in PASMC isolated from rats with PH correlates with deficiencies in the activities of Complexes I, II and III. We also identified increases in mitochondrial reactive oxygen species generation and mitochondrial membrane potential. The defect in Complex I activity correlates with a loss in its assembly, although the assembly of Complexes II and III are both maintained.

2. Methods

2.1. Animals

A total of 110 male Sprague Dawley rats (SD; 220–270 g) were used in this study ($n=5$–10 per group). Animals were housed in the Georgia Regents University animal care facility for at least 1 week before being used in the experiments. Animals were kept in a 12-h light/dark cycle at an ambient temperature of 22 °C and received standard rodent food and water ad libitum. All experimental procedures were approved by the Institutional Animal Care and Use Committee at Georgia Regents University. Monocrotaline rats received either a single injection of vehicle (Control group) or monocrotaline (60 mg/kg, MCT group) to induce pulmonary hypertension (PH). All animals were sacrificed 28 days after injection.

2.2. Smooth muscle cells (SMC) isolation

Rats were sacrificed, and the heart and lung are removed in one piece. The lobes of the lung were then separated into whole pieces in preparation for removal of the main pulmonary artery. The main pulmonary artery was then removed, opened and gently swabbed to remove the endothelial cells. The denuded vessels were then cut into small pieces and added to an enzyme solution consisting of 37 mg of collagenase type 2 (Worthington) and 125 mg of BSA in 10 ml of dissociation buffer. Vessels were then incubated for 30 min at 37 °C. After enzyme digestion, the samples were removed and vigorously vortexed. Cells were then precipitated by centrifugation at 2000*g* for 10 min. The resulting pellet was then resuspended in 3 ml of 10% FBS DMEM medium containing an antibiotic/antifungal solution. Cells were confirmed as SMC by staining with smooth muscle cell actin. Cells were plated for 7 days then reseeded for Seahorse XF experiments or harvested for mitochondrial isolation.

2.3. Mitochondrial bioenergetics

The XF24 Analyzer (Seahorse Biosciences, North Billerica, MA, USA) was used to measure changes in mitochondrial bioenergetics by measuring the oxygen consumption rate (OCR). PASMC were plated on XF24 culture microplates. The optimum number of PASMC/well was determined to be 40,000/0.32 cm^2. Dulbecco's modified Eagle's medium (DMEM, pH 7.4) supplemented with 5 mM glucose and 2 mM sodium pyruvate was then added. The plates were then incubated in a CO_2-free XF prep station at 37 °C for 40 min to allow temperature and pH calibration. We then sequentially injected Oligomycin (1 μm final concentration); an ATP synthase inhibitor, which decreases OCR levels, followed by FCCP (carbonyl cyanide 4- (trifluoromethoxy) phenylhydrazone, 1 μm final concentration); an electron transport chain accelerator which causes maximal respiration and finally Rotenone+antimycin A (1 μm final concentration of each) which are mitochondrial Complex 1 and III inhibitors, respectively. Subsequently, the mitochondrial respiratory parameters were calculated from the OCR values. All the OCR values were expressed in pmoles/min of oxygen consumed. All the drugs were used from the XF Cell Mito Stress Test Kit (# 101706-100; Seahorse Biosciences). Reserve capacity was calculated as the difference in between basal OCR and that obtained in the presence of FCCP. Maximal respiratory capacity was determined as the difference in OCR between Rotenone+Antimycin A and FCCP.

2.4. Analysis of cellular glycolysis

To estimate changes in cellular glycolytic rates we measured changes in the extracellular acidification rate (ECAR). PASMC were glucose-starved in XF assay medium in a CO_2-free XF prep station at 37 °C for 40 min and then sequentially injected with glucose (2 mg/ml), oligomycin (1 μM) and 2-deoxy-D-glucose (100 mM). Differences in basal-, maximal- and spare glycolytic capacity were then determined and the data represented as mpH/min. Spare glycolytic capacity was determined as the difference in ECAR between basal ECAR and that obtained in the presence of oligomycin.

2.5. Respiratory chain complex functional analysis in permeabilized pulmonary arterial smooth muscle cells

Cells were seeded in an XF24 cell culture microplate at 20,000 cells per well two days before the initiation of the experiment. On the days of the experiment, cells were washed with 1 × MAS buffer (Mannitol 220 mM, Sucrose 70 mM, KH_2PO_4 10 mM, $MgCl_2$ 5 mM, HEPES 2 mM, EGTA 1 mM, Fatty Acid Free (FAF) BSA 0.2% (w/v)). A Pyruvate/Malate/ADP (10 mM/1 mM/4 mM respectively) mixture was added to the MAS buffer to form the assay medium. Prior to starting the assay, mitochondrial Complex substrates and inhibitors, in 1 × MAS buffer, were added to the injection ports of the cartridge: Port 1: Complex I inhibitor – rotenone (2 μM), Port 2: Complex II substrate – succinate (10 mM) or the Complex III substrate-tetramethyl-hydroquinone (0.5 mM), Port 3: Complex V inhibitor – oligomycin (1 μM). Cells were then treated with plasma membrane permeabilizer (1 nM XF PMP (Seahorse Biosciences), final volume of 0.5 ml per well) mixed with assay medium to initiate the experiment and immediately transfered to the XF24 analyzer. Initial readings were used to determine the basal OCR of respiring mitochondria (Stage 1). To determine the Complex I component of the OCR, the Complex I inhibitor, rotenone (2 μM) was injected (Stage 2). The difference in OCR between Stage 1 and 2 was attributed to the respiratory activity of Complex I. The Complex II substrate, succinate, was then injected to activate electron flow through Complex II, and bypass the need for Complex I (Stage 3). The difference in OCR between Stage 2 and 3 was

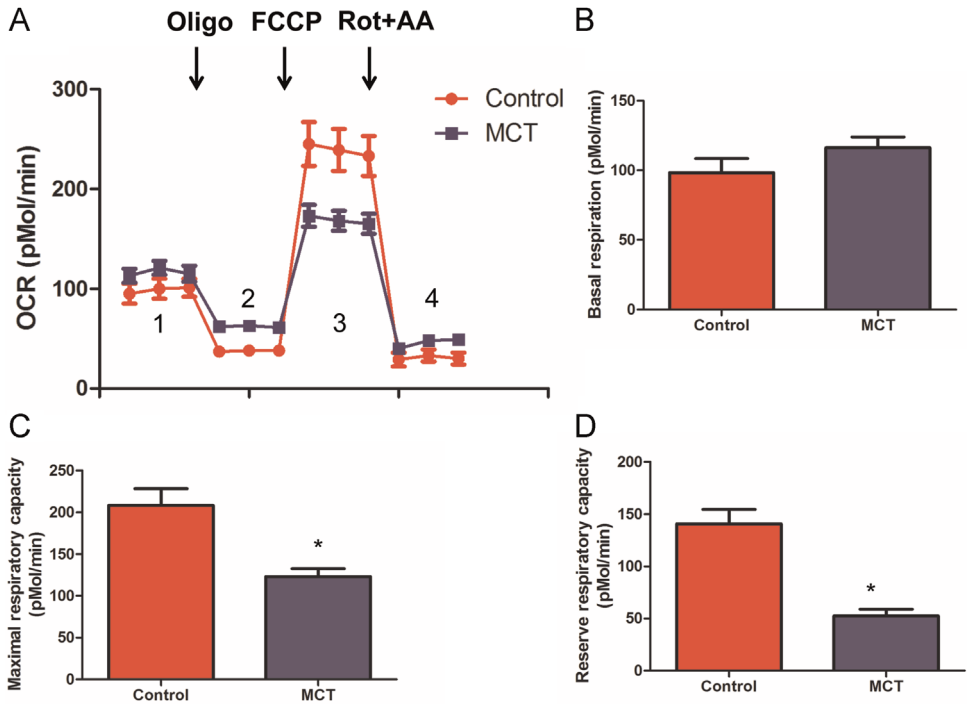

Fig. 1. Mitochondrial respiration is attenuated in pulmonary arterial smooth muscle cells isolated from rats with pulmonary hypertension. The Seahorse XF24 analyzer was used to take measurements in PASMC (40,000/0.32 cm^2) isolated from control (red) and PH (blue) rats. Oligomycin (1 μM), FCCP (1 μM), and Rotenone and Antimycin A (1 μM each) were added at the indicated points (A). Basal mitochondrial respiration (B) is unchanged between control and PH-PASMC as estimated by measuring the rate of oxygen consumption rate (OCR, pmols/min). Both the maximal respiratory capacity (C) and the reserve respiratory capacity (D) are significantly attenuated in PH-PASMC. Values are means ± SEM. *($p < 0.05$ vs. Control PH-PASMC, $N = 10$ measurements from 3 independent SMC isolations). (For interpretation of the references to color in this figure legend,the reader is referred to the web version of this article.)

attributed to the respiratory activity of Complex II. In a different set of studies, Complex III activity was stimulated by the injection of tetramethyl-hydroquinone (0.5 mM) after the injection of rotenone (Stage 3). Again the difference in OCR between Stage 2 and 3 was attributed to the respiratory activity of Complex III. In both studies, as a last challenge, oligomycin was injected to attenuate ATP synthase activity (Stage 4). This served as a control to ensure that mitochondrial respiration was being measured. In the assay we utilized mix/wait/measure times of 0.5 min/0.5 min/2 min with no equilibration step and took 2 measurements per step.

2.6. Determination of mitochondrial ROS levels

MitoSOX™ Red mitochondrial superoxide indicator (Molecular Probes, Grand Island, NY) a fluorogenic dye for selective detection of superoxide in the mitochondria of live cells was used. Briefly, cells were washed with fresh media, and then incubated in media containing MitoSOX Red (2 μM), for 30 min at 37 °C in dark conditions then subjected to fluorescence microscopy at an excitation of 510 nm and an emission at 580 nm. An Olympus IX51 microscope equipped with a CCD camera (Hamamatsu Photonics) was used for acquisition of fluorescent images. The average fluorescent intensities (to correct for differences in cell number) were quantified using ImagePro Plus version 5.0 imaging software (Media Cybernetics).

2.7. Analysis of mitochondrial membrane potential

Mitochondrial membrane potential was determined using tetramethylrhodamine methyl ester perchlorate, TMRM (Molecular Probes, Eugene, OR). Briefly, cells were washed with fresh media, and incubated in media containing TMRM (50 nM), for 30 min at 37 °C in dark conditions then subjected to fluorescence microscopy at an excitation of 510 nm and an emission at 580 nm. An Olympus IX51 microscope equipped with a CCD camera (Hamamatsu Photonics) was used for acquisition of fluorescent images. The average fluorescent intensities (to correct for differences in cell number) were quantified using ImagePro Plus version 5.0 imaging software (Media Cybernetics).

2.8. Mitochondrial isolation and analysis of electron chain complexes

Mitochondria from PASMC were isolated using the Pierce Mitochondria isolation kit for cultured cells (Pierce, Rockford, IL) as previously described [13]. Pelleted mitochondria samples were solubilized in cold 1X NativePAGE™ Sample Buffer (Life technologies) containing 1% n-dodecyl-β-D-maltoside (DDM) and 1% Digitonin and mixed by pipetting up and down. Samples were incubated on ice for 15 min, and then centrifuged at 20,000 × *g* for 30 min at 4 °C. Samples were loaded in wells filled with 1X NativePAGE™ Dark Blue Cathode Buffer prior to filling the cathode chamber to better visualize the sample wells. The upper Cathode Buffer Chamber was filled with 200 mL 1 × NativePAGE™ Dark Blue Cathode Buffer, and the Lower Anode Buffer Chamber filled with 550 mL NativePAGE™ Anode Buffer. Electrophoresis was run for 120 min at 150 V.

2.9. Statistical analysis

Statistical analysis was performed using GraphPad Prism version 4.01 for Windows (GraphPad Software). The mean ± SEM were calculated for all samples and significance was determined by the unpaired *t*-test. A value of $p < 0.05$ was considered significant.

3. Results

3.1. Disrupted bioenergetics in pulmonary arterial smooth muscle

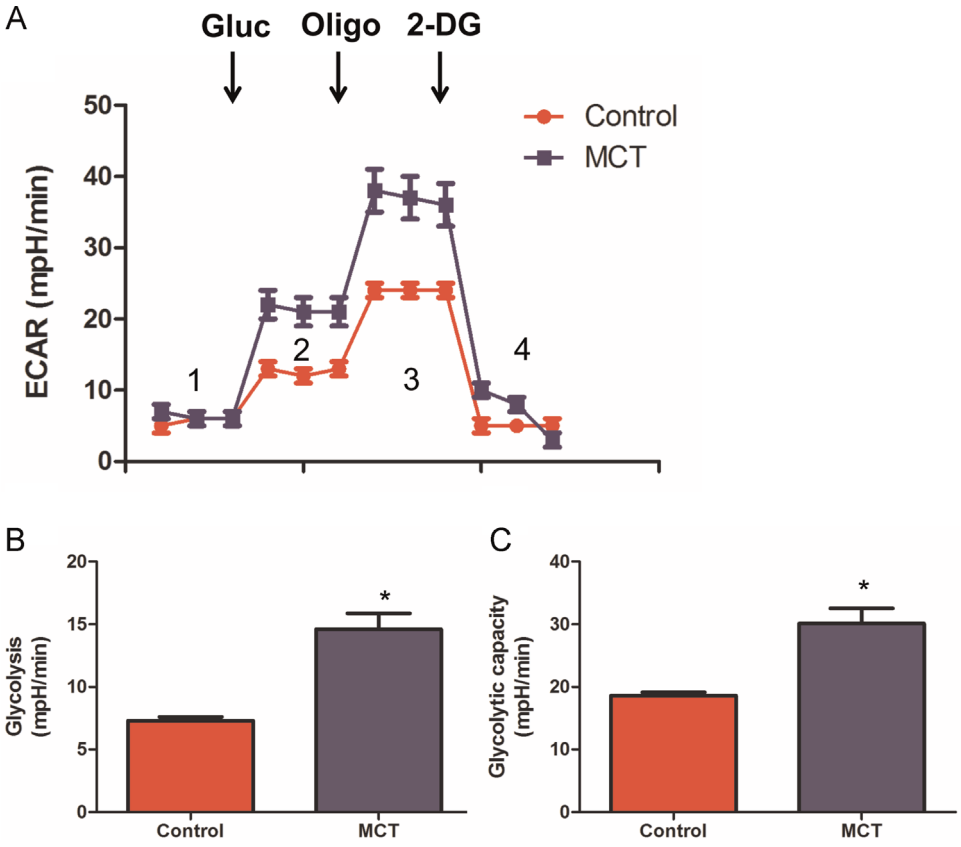

Fig. 2. Glycolysis is increased in pulmonary arterial smooth muscle cells isolated from rats with pulmonary hypertension. The Seahorse XF24 analyzer was used to take extracellular acidification rate (ECAR) measurements in PASMC (20,000/0.32 cm^2) isolated from control (red, $N=10$) and PH (blue, $N=10$) rats. D-glucose (2 mg/ml), oligomycin (1 μM) and 2-deoxy-D-glucose (100 mM) were added at the indicated points (A). There is no difference in the glycolytic rate between control and PH-PASMC in the absence of substrate (B). However, the addition of D-glucose caused a significant increase in ECAR in PH- compared to Control-PASMC (C). The addition of oligomycin increased ECAR significantly more in PH- compared to control-PASMC (D). Values are means ± SEM. *($p < 0.05$ vs. Control PH-PASMC, $N=10$ measurements from 3 independent SMC isolations). (For interpretation of the references to color in this figure legend,the reader is referred to the web version of this article.)

cells isolated from rats with pulmonary hypertension

In PASMC isolated from control and MCT-treated rats, oxygen consumption rates were monitored (Fig. 1A). Our data identified a similar level of basal respiration between control- and PH-PASMC (Fig. 1B). Interestingly, the decrease in OCR in control PASMC exposed to oligomycin was significantly greater than that in the PH PASMC. This may reflect additional non-mitochondrial oxygen consumption in the PH cells. In addition, both spare and maximal respiratory capacities were significantly reduced in PASMC isolated from rats with PH (Fig. 1C and D).

3.2. Increased glycolysis in pulmonary arterial smooth muscle cells isolated from rats with pulmonary hypertension

In PASMC isolated from contro–l and MCT-treated rats, acidification rates were monitored to estimate glycolysis. Our data identified a similar level of basal acidification between control- and PH-PASMC (Fig. 2A). After challenge with glucose the acidification rate was significantly higher in PH-PASMC (Fig. 2B). Our data also indicate that maximal glycolytic rate is significantly higher in PH-PASMC (Fig. 2C). The glycolysis inhibitor, 2-deoxy-D-glucose reduced the acidification rate in both control- and PH-PASMC (Fig. 2A).

3.3. The activities of complex I, II and III are reduced in pulmonary arterial smooth muscle cells isolated from rats with pulmonary hypertension

To understand the role of mitochondrial respiratory chain Complexes in mitochondrial dysfunction and glycolytic switch, we utilized a novel cell permeabilization protocol to allow us to measure individual Complex activity in cells. Our data indicate that the activities of both Complex I and Complex II are decreased by ~50% in PH-PASMC (Fig. 3). Unfortunately, the Seahorse XF instrument is limited to 4 injections, so, we could not examine substrate utilization from all mitochondrial Complexes in a single experiment. Thus, in a separate set of experiments, we measured Complex I and Complex III activity. Our data indicate that Complex III activity is also inhibited by ~50% in PH-PASMC (Fig. 4). Interestingly, this 50% reduction in Complex I–III activity correlates well with the ~50% decrease in overall mitochondrial OCR (Fig. 1).

3.4. Mitochondrial ROS generation and membrane potential are increased in pulmonary arterial smooth muscle cells isolated from rats with pulmonary hypertension

Our data indicate that PASMC from MCT-treated rats have significantly increased mitochondrial ROS production (Fig. 5). This observation correlates well with our finding of respiratory chain dysregulation in PH rats, as more electrons can escape between Complexes and become trapped in oxygen, potentially increasing superoxide levels in the mitochondria. The mitochondrial membrane potential is also increased in PASMC from MCT-treated rats (Fig. 6). This result is surprising in the context of reduced activity of Complexes I–III, all of which maintain membrane potential, in

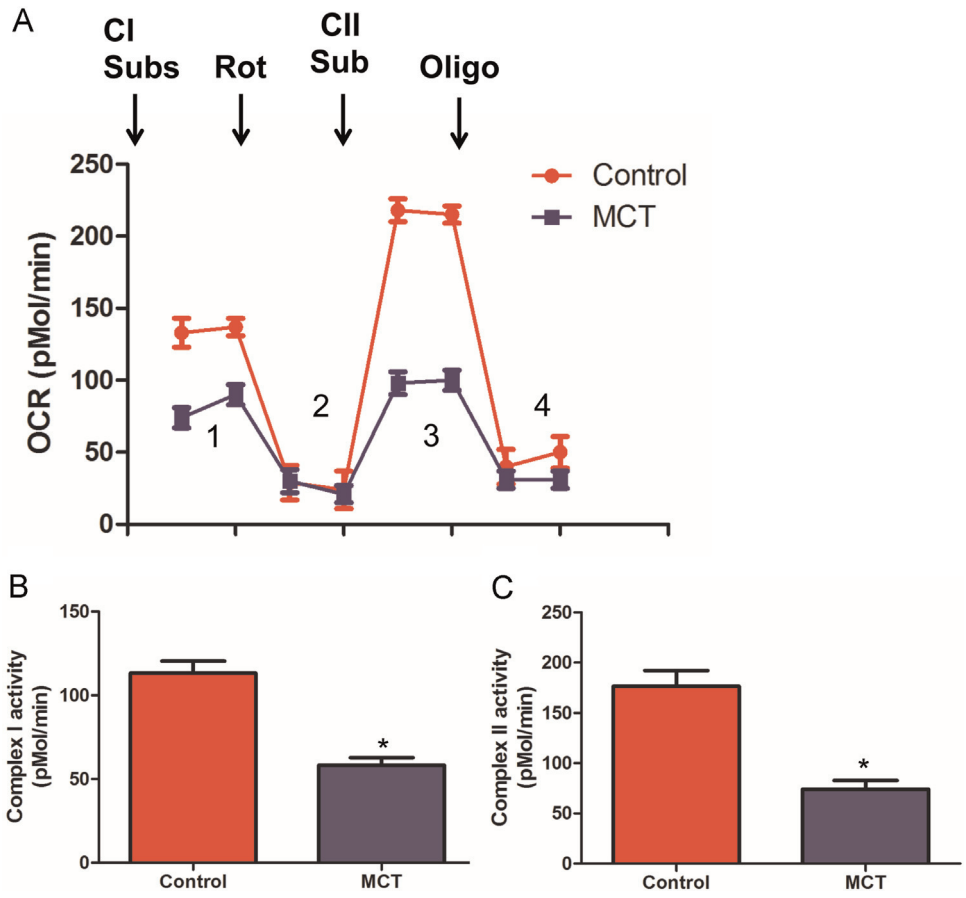

Fig. 3. Complex I and Complex II dependent respiration is attenuated in pulmonary arterial smooth muscle cells isolated from rats with pulmonary hypertension. The Seahorse XF24 analyzer was used to take OCR measurements in PASMC (40,000/0.32 cm^2) isolated from control (red) and PH (blue) rats to determine Complex I and II respiratory activity (A). Both Complex I (B) and Complex II (C) activities are attenuated in PH- compared to Control-PASMC. Values are means ± SEM. *($p < 0.05$ vs. Control PH-PASMC, $N = 5–15$ measurements from 3 independent SMC isolations). (For interpretation of the references to color in this figure legend,the reader is referred to the web version of this article.)

PASMC from MCT-treated rats.

3.5. Loss of complex I assembly in pulmonary arterial smooth muscle cells isolated from rats with pulmonary hypertension

In order to evaluate individual intact Complexes we utilized native blue gel electrophoresis on isolated fresh mitochondria from control- and PH-PASMC. Our data indicate that PASMC isolated from PH rats have a marked loss of Complex I (Fig. 7). However, we found that Complex II remained unchanged and Complex III was significantly elevated in PH-PASMC. This finding contradicts with our data demonstrating that Complex II and III activities are both decreased in PH-PASMC (Figs. 3 and 4). One possible explanation is that the uncoupling of electron transport chain due to derangements in Complex I prevents Complex II and III from transporting electrons effectively. However, the increased levels of Complex III may explain the increase in mitochondrial membrane potential we observe in PH-PASMC (Fig. 6).

4. Discussion

Our data suggest that the mitochondrial dysfunction in associated with PH occurs via a loss of Complex I assembly and Complex I activity. Our data also suggest that Complex I dysregulation appears to lead to the inhibition of Complexes II and III. The mitochondrial electron transfer chain consists of five distinct Complexes [14]. Complex I is the largest enzyme and plays critical roles both in transferring electrons from reduced NADH to Coenzyme Q and in maintaining the proton electrochemical gradient across the inner mitochondrial membrane [14]. Complex I contains a large number of different subunits (45) that are all required for catalytic function and are conserved across different species. The core of Complex I is assembled by 14 subunits [15]. Seven subunits are encoded by mitochondrial DNA and seven are encoded by nuclear DNA [15]. The mitochondrial derived subunits play an important role in proton pumping from the matrix, whereas the non-mitochondrial subunits are involved in electron transfer [16]. Electrons flowing from NADH to Coenzyme Q induces proton translocation across the mitochondrial membrane secondary to conformational changes in the membrane arm of Complex I [17]. Two electrons pump four protons and this contributes to the electrochemical gradient that drives further ATP synthesis. The function of the other 31 subunits is largely unexplored due to instability and the trans-membrane nature of Complex I. However, these functions are likely involved in the assembly and stabilization of the multimeric Complex, regulation of activity, and protection against reactive oxygen species. Mutations that affect Complex I assembly lead to severe childhood diseases. For example, fatal infantile lactic acidosis [18] is a fatal Complex I deficiency disorder, linked to mutations in several nuclear-encoded subunits. This disease is characterized by lactate buildup in the body due to the inability to process pyruvate via oxidative phosphorylation. Leigh syndrome, characterized with respiratory abnormalities, nystagmus, ataxia, dystonia and hypotonia, is the most frequent presentation of Complex I deficiency [19,20], also

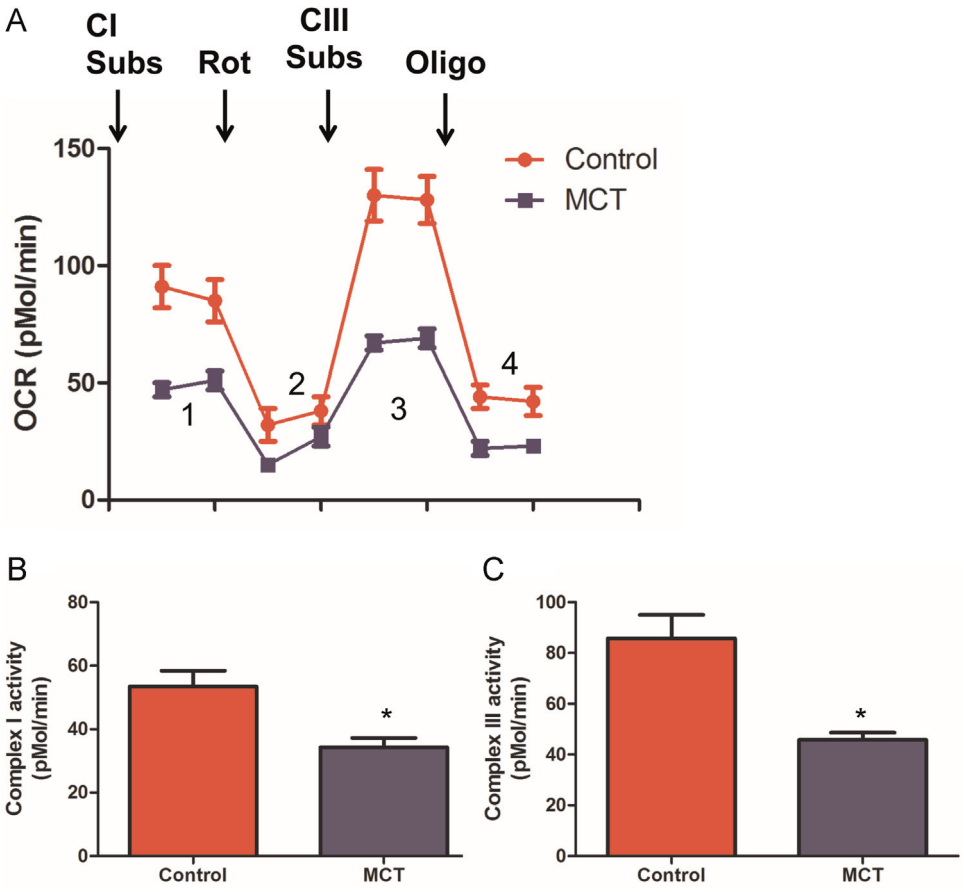

Fig. 4. Complex III dependent respiration is attenuated in pulmonary arterial smooth muscle cells isolated from rats with pulmonary hypertension. The Seahorse XF24 analyzer was used to take OCR measurements in PASMC (40,000/0.32 cm^2) isolated from control (red) and PH (blue) rats to determine Complex I and III respiratory activity (A). Both Complex I (B) and Ccomplex III (C) activities are attenuated in PH- compared to Control-PASMC. Values are means ± SEM. *($p < 0.05$ vs. Control PH-PASMC, $N = 10$ measurements from 3 independent SMC isolations). (For interpretation of the references to color in this figure legend,the reader is referred to the web version of this article.)

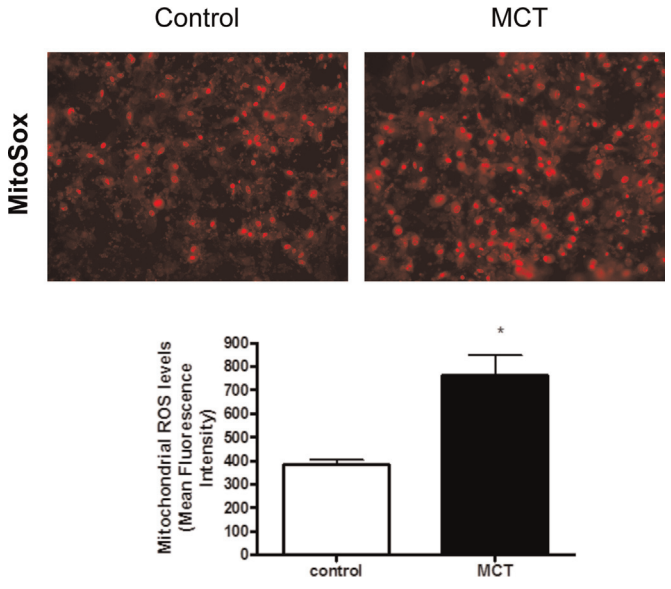

Fig. 5. Mitochondrial ROS production is increased in pulmonary arterial smooth muscle cells isolated from rats with pulmonary hypertension. PASMC were pre-incubated with the mitoSOX red fluorescent dye. Digital images of mitoSOX fluorescence were obtained by fluorescent microscopy. Representative digital images from PASMC isolated from control and PH rats SMC are shown. Quantification of the fluorescent signal indicates that ROS production is increased in PH-PASMC. Data are plotted as mean fluorescence intensity (± SEM). *($p < 0.05$, $N = 10$).

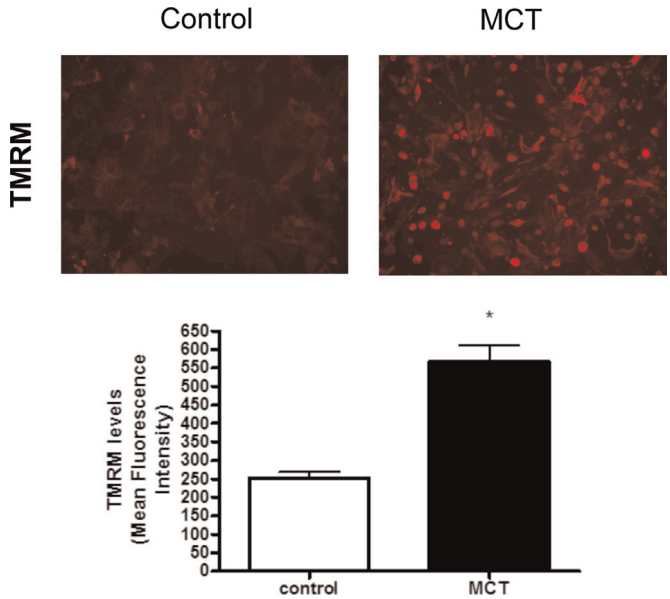

Fig. 6. Mitochondrial membrane potential is increased in pulmonary arterial smooth muscle cells isolated from rats with pulmonary hypertension. PASMC were pre-incubated with TMRM to polarized mitochondria. Digital images of TMRM fluorescence were obtained using fluorescent microscopy. Representative digital images from PASMC isolated from control and PH rats SMC are shown. Quantification of the fluorescent signal indicates that the mitochondrial membrane potential is increased in PH-PASMC. Data are plotted as mean fluorescence intensity (± SEM). *($p < 0.05$, $N = 10$).

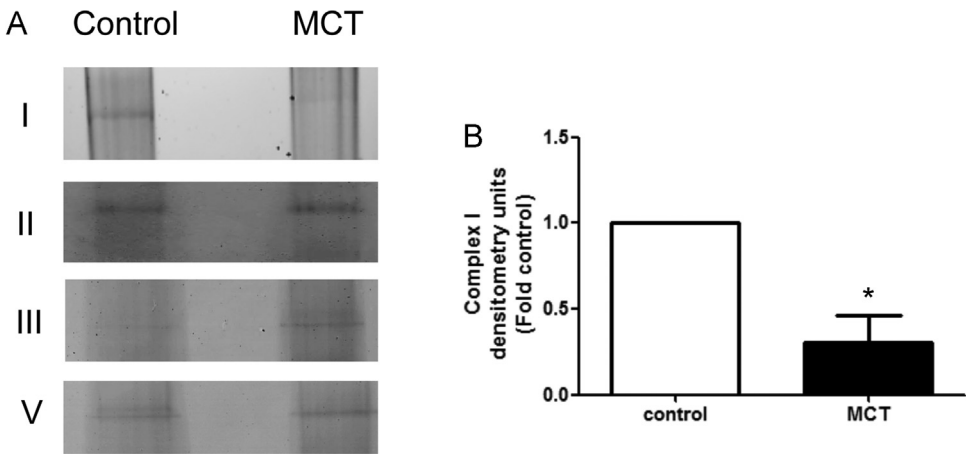

Fig. 7. Complex I assembly is attenuated in pulmonary arterial smooth muscle cells isolated from rats with pulmonary hypertension. Mitochondria, obtained from PASMC isolated from control and PH rats SMC, were subjected to Native Blue electrophoresis to preserve the respiratory Complexes (A). Complex I levels are significantly reduced in PH-PASMC (B). Complex II and V levels are unchanged and Complex III levels are increased in PH-PASMC. The image shown is representative of three independent SMC isolations experiments. Data are plotted as mean ± SEM, $^{*}p < 0.05$.

associated with elevated lactate levels fluid [21]. Although any oxidative phosphorylation Complexes defect can contribute to Leigh syndrome, Complex I deficiency is the primary cause of the disease. Mutations in six mitochondrial and eleven nuclear encoded Complex I subunits and several assembly factors have been linked with Leigh syndrome [22].

The inhibition of Complex II and III, likely as result of reduced Complex I activity, occurred despite the fact that Complex II protein levels were similar between control and PH PASMC and Complex III levels were elevated in the PH cells. Thus, changes in protein levels do not appear to explain the loss of function we identified in Complex II and III. However, it has been shown that the majority of Complex I exists within respiratory chain supercomplexes or 'respirasomes' that are composed of Complex I, Complex III, and Complex IV [23]. These supercomplexes appear to have functional advantages, including increased efficacy of electron-, proton- and substrate flow, as well as stabilization and protection from degradation [24,25]. Overall this decreases electron leak that can lead to the formation of reactive oxygen species (ROS) as well as proton leak [26]. It has been further suggested that Complex I assembly is required for supercomplex formation [27]. Moreover, the requirement for supercomplex formation to allow efficient electron transport chain function may explain the dysfunction that has been identified in other complexes associated with Complex I mutations; for example, Complex III defects have been identified in some patients with NDUFS4 subunit mutations [28,29] and Complex IV deficiency [30] has been found in some patients with defects in the Complex I assembly factor, C20ORF7.17 [31]. Thus, the need for suplercomplex formation may explain why derangements in Complex I in PH-PASMC lead to dysfunction of other respiratory chain complexes.

Complex I is also an important site for the generation of ROS and the electrochemical gradient. Paradoxically, we found that the loss of Complex I activity was associated with increased ROS production and increased mitochondrial membrane potential. As Complex III is another major site of ROS production and proton exchange, our observed increase in Complex III in PH-PASMC may compensate for the loss of Complex I and contribute to the increase in both ROS and the mitochondrial potential. While Complexes I and III are thought to generate most of the mitochondrial ROS [32], heterogeneity in the amount of these Complexes within the mitochondria also determines their individual importance. Thus, ROS generation is predominantly from Complex III in hypoxic myocytes [33], while Complex II has been shown to be the predominant source in the hypoxic lung [34]. Further, Complex II activity is increased in the right ventricle in the MCT rat model of PH and is the major ROS generator [35]. However, in PH the role of mitochondrial derived ROS is controversial with competing studies suggesting that mitochondrial ROS can either increase or decrease. Decreased levels of mitochondrial derived ROS have been found in PASMC isolated from humans with PH [36], the fawn hooded rat [37], and hypoxia-, and MCT-induced PH [38]. While mitochondrial ROS have been shown to be increased in PH associated with PPARγ inhibition [39] and in PAEC exposed to ET-1 [11] or ADMA [10]. Although more work is clearly needed to clarify the role of mitochondrial ROS in the development of PH, it is reasonable to conclude that the PH field has reached a consensus that the mitochondria play an important role in the development of PH.

Our data also confirm previous studies that vascular cells in PH exhibit an increase in aerobic glycolysis. This glycolytic switch was first hypothesized in the 1920's by Otto Warburg, as a mechanism that gives a proliferative advantage to cancer cells [40]. The hypoxic microenvironment around tumors appears to stimulate the metabolic switch to glycolysis [41]. Interestingly, some animal models of PH utilize hypoxia as an inducer. PH is also characterized by the tumor-like growth of vascular wall cells. Therefore, the metabolic switch in PH may also be induced by hypoxia. Hypoxia inducible factor (HIF) is known to activate survival genes that are linked to cellular adaptation to hypoxia [42]. For example, HIF induces vascular endothelial growth factor (VEGF), hepatocyte growth factor receptor (c-Met), erythropoietin, transforming growth factor-α (TGF-α), platelet-derived growth factor-β (PDGF-β) and glucose transporter GLUT1, and is thus able to influence many cellular activities, including angiogenesis, glycolysis and cell survival [43]. HIF also plays a critical role in shifting ATP generation from oxidative phosphorylation to glycolysis. This appears to be dependent on mammalian target of rapamycin (mTOR) activation via Akt signaling [44]. We have recently reported that Akt1 signaling can be enhanced through a single nitration at Y350 [13]. This, in turn, leads to mitochondrial dysfunction secondary to the mitochondrial redistribution of eNOS followed by the downstream activation of HIF [11]. As nitration is increased in multiple models of PH [45–51] it is possible that this type of Akt1 activation [52] may be shifting the cellular metabolic state by inhibiting mitochondrial respiration and activating glycolysis at the same time. However, this is a speculation and more work will be required to unravel the mechanisms by which the glycolytic switch occurs during the development of PH.

In conclusion, our data suggest that, in PASMC isolated from PH

rats, derangements in Complex I can also reduce the activity of Complex II and III in the ETC. This appears to have effects on the activity of downstream respiratory chain complexes as well as mitochondrial ROS generation and membrane potential. There is also a compensatory metabolic switch to glycolysis for ATP generation. Similar to tumor growth, this metabolic reprogramming likely leads PASMC proliferation and vascular remodeling. We speculate that therapies targeted at restoring Complex I activity could have potential in the treatment of PH.

Acknowledgments

This research was supported in part by National Institutes of Health Grants HL60190, HL67841, and P01HL0101902 (to SMB), HL61284 (to JRF), an Entelligence Actelion Young Investigator Award for Research Excellence in Pulmonary Hypertension and by F32HL10313 (to OR), and a Scientist Development Grant (14SDG20480354) from the American Heart Association National Office (to RR).

References

[1] G.K. Owens, M.S. Kumar, B.R. Wamhoff, Molecular regulation of vascular smooth muscle cell differentiation in development and disease, Physiol. Rev. 84 (2004) 767–801.
[2] H. Hao, G. Gabbiani, M.L. Bochaton-Piallat, Arterial smooth muscle cell heterogeneity: implications for atherosclerosis and restenosis development, Arterioscler. Thromb. Vasc. Biol. 23 (2003) 1510–1520.
[3] T.M. Lincoln, N.B. Dey, N.J. Boerth, T.L. Cornwell, G.A. Soff, Nitric oxide-cyclic GMP pathway regulates vascular smooth muscle cell phenotypic modulation: implications in vascular diseases, Acta Physiol. Scand. 164 (1998) 507–515.
[4] S. Negash, S.R. Narasimhan, W. Zhou, J. Liu, F.L. Wei, J. Tian, J.U. Raj, Role of cGMP-dependent protein kinase in regulation of pulmonary vascular smooth muscle cell adhesion and migration: effect of hypoxia, Am. J. Physiol.: Heart Circ. Physiol. 297 (2009) H304–H312.
[5] W. Zhou, S. Negash, J. Liu, J.U. Raj, Modulation of pulmonary vascular smooth muscle cell phenotype in hypoxia: role of cGMP-dependent protein kinase and myocardin, Am. J. Physiol. Lung Cell. Mol. Physiol. 296 (2009) L780–L789.
[6] S.L. Archer, G. Marsboom, G.H. Kim, H.J. Zhang, P.T. Toth, E.C. Svensson, J. R. Dyck, M. Gomberg-Maitland, B. Thebaud, A.N. Husain, N. Cipriani, J. Rehman, Epigenetic attenuation of mitochondrial superoxide dismutase 2 in pulmonary arterial hypertension: a basis for excessive cell proliferation and a new therapeutic target, Circulation 121 (2010) 2661–2671.
[7] J. Rehman, S.L. Archer, A proposed mitochondrial-metabolic mechanism for initiation and maintenance of pulmonary arterial hypertension in fawn-hooded rats: the Warburg model of pulmonary arterial hypertension, Adv. Exp. Med. Biol. 661 (2010) 171–185.
[8] F.A. Masri, W. Xu, S.A. Comhair, K. Asosingh, M. Koo, A. Vasanji, J. Drazba, B. Anand-Apte, S.C. Erzurum, Hyperproliferative apoptosis-resistant endothelial cells in idiopathic pulmonary arterial hypertension, Am. J. Physiol. Lung Cell. Mol. Physiol. 293 (2007) L548–L554.
[9] W. Xu, T. Koeck, A.R. Lara, D. Neumann, F.P. DiFilippo, M. Koo, A.J. Janocha, F. A. Masri, A.C. Arroliga, C. Jennings, R.A. Dweik, R.M. Tuder, D.J. Stuehr, S. C. Erzurum, Alterations of cellular bioenergetics in pulmonary artery endothelial cells, Proc. Natl. Acad. Sci. U.S.A. 104 (2007) 1342–1347.
[10] X. Sun, S. Sharma, S. Fratz, S. Kumar, R. Rafikov, S. Aggarwal, O. Rafikova, Q. Lu, T. Burns, S. Dasarathy, J. Wright, C. Schreiber, M. Radman, J.R. Fineman, S. M. Black, Disruption of endothelial cell mitochondrial bioenergetics in lambs with increased pulmonary blood flow, Antioxid. Redox Signal. 18 (2013) 1739–1752.
[11] X. Sun, S. Kumar, S. Sharma, S. Aggarwal, Q. Lu, C. Gross, O. Rafikova, S.G. Lee, S. Dasarathy, Y. Hou, M.L. Meadows, W. Han, Y. Su, J.R. Fineman, S.M. Black, Endothelin-1 induces a glycolytic switch in pulmonary arterial endothelial cells via the mitochondrial translocation of endothelial nitric oxide synthase, Am. J. Respir. Cell Mol. Biol. 50 (2014) 1084–1095.
[12] J. Rehman, S.L. Archer, A proposed mitochondrial-metabolic mechanism for initiation and maintenance of pulmonary arterial hypertension in fawn-hooded rats: the Warburg model of pulmonary arterial hypertension, Adv. Exp. Med. Biol. 661 (2010) 171–185.
[13] R. Rafikov, O. Rafikova, S. Aggarwal, C. Gross, X. Sun, J. Desai, D. Fulton, S. M. Black, Asymmetric dimethylarginine induces endothelial nitric-oxide synthase mitochondrial redistribution through the nitration-mediated activation of Akt1, J. Biol. Chem. 288 (2013) 6212–6226.
[14] M. Mimaki, X. Wang, M. McKenzie, D.R. Thorburn, M.T. Ryan, Understanding mitochondrial complex I assembly in health and disease, Biochim. Biophys. Acta 1817 (2012) 851–862.
[15] J. Hirst, J. Carroll, I.M. Fearnley, R.J. Shannon, J.E. Walker, The nuclear encoded subunits of complex I from bovine heart mitochondria, Biochim. Biophys. Acta 1604 (2003) 135–150.
[16] S. Drose, S. Krack, L. Sokolova, K. Zwicker, H.D. Barth, N. Morgner, H. Heide, M. Steger, E. Nubel, V. Zickermann, S. Kerscher, B. Brutschy, M. Radermacher, U. Brandt, Functional dissection of the proton pumping modules of mitochondrial complex I, PLoS Biol. 9 (2011) e1001128.
[17] E.A. Baranova, P.J. Holt, L.A. Sazanov, Projection structure of the membrane domain of Escherichia coli respiratory complex I at 8A resolution, J. Mol. Biol. 366 (2007) 140–154.
[18] C.L. Hoppel, D.S. Kerr, B. Dahms, U. Roessmann, Deficiency of the reduced nicotinamide adenine dinucleotide dehydrogenase component of complex I of mitochondrial electron transport. Fatal infantile lactic acidosis and hypermetabolism with skeletal–cardiac myopathy and encephalopathy, J. Clin. Invest. 80 (1987) 71–77.
[19] A. Quintana, S.E. Kruse, R.P. Kapur, E. Sanz, R.D. Palmiter, Complex I deficiency due to loss of Ndufs4 in the brain results in progressive encephalopathy resembling Leigh syndrome, Proc. Natl. Acad. Sci. U.S.A. 107 (2010) 10996–11001.
[20] R.H. Triepels, L.P. van den Heuvel, J.L. Loeffen, C.A. Buskens, R.J. Smeets, M. E. Rubio Gozalbo, S.M. Budde, E.C. Mariman, F.A. Wijburg, P.G. Barth, J. M. Trijbels, J.A. Smeitink, Leigh syndrome associated with a mutation in the NDUFS7 (PSST) nuclear encoded subunit of complex I, Ann. Neurol. 45 (1999) 787–790.
[21] P.F. Chinnery, in: R.A. Pagon, M.P. Adam, H.H. Ardinger, S.E. Wallace, A. Amemiya, L.J.H. Bean, T.D. Bird, C.R. Dolan, C.T. Fong, R.J.H. Smith, K. Stephens (Eds.), Mitochondrial Disorders Overview, GeneReviews®, Seattle, WA, 1993.
[22] W.J. Koopman, F. Distelmaier, J.A. Smeitink, P.H. Willems, OXPHOS mutations and neurodegeneration, EMBO J. 32 (2013) 9–29.
[23] H. Schagger, Respiratory chain supercomplexes of mitochondria and bacteria, Biochim. Biophys. Acta 1555 (2002) 154–159.
[24] J.N. Blaza, R. Serreli, A.J. Jones, K. Mohammed, J. Hirst, Kinetic evidence against partitioning of the ubiquinone pool and the catalytic relevance of respiratory-chain supercomplexes, Proc. Natl. Acad. Sci. U.S.A. 111 (2014) 15735–15740.
[25] G. Lenaz, M.L. Genova, Structural and functional organization of the mitochondrial respiratory chain: a dynamic super-assembly, Int. J. Biochem. Cell Biol. 41 (2009) 1750–1772.
[26] G. Lenaz, M.L. Genova, Structure and organization of mitochondrial respiratory complexes: a new understanding of an old subject, Antioxid. Redox Signal. 12 (2010) 961–1008.
[27] G. Lenaz, A. Baracca, R. Fato, M.L. Genova, G. Solaini, Mitochondrial Complex I: structure, function, and implications in neurodegeneration, Ital. J. Biochem. 55 (2006) 232–253.
[28] S. Scacco, V. Petruzzella, S. Budde, R. Vergari, R. Tamborra, D. Panelli, L.P. van den Heuvel, J.A. Smeitink, S. Papa, Pathological mutations of the human NDUFS4 gene of the 18-kDa (AQDQ) subunit of complex I affect the expression of the protein and the assembly and function of the complex, J. Biol. Chem. 278 (2003) 44161–44167.
[29] S.M. Budde, L.P. van den Heuvel, A.J. Janssen, R.J. Smeets, C.A. Buskens, L. DeMeirleir, R. Van Coster, M. Baethmann, T. Voit, J.M. Trijbels, J.A. Smeitink, Combined enzymatic complex I and III deficiency associated with mutations in the nuclear encoded NDUFS4 gene, Biochem. Biophys. Res. Commun. 275 (2000) 63–68.
[30] S. Scacco, V. Petruzzella, E. Bertini, A. Luso, F. Papa, F. Bellomo, A. Signorile, A. Torraco, S. Papa, Mutations in structural genes of complex I associated with neurological diseases, Ital. J. Biochem. 55 (2006) 254–262.
[31] A. Saada, S. Edvardson, A. Shaag, W.K. Chung, R. Segel, C. Miller, C. Jalas, O. Elpeleg, Combined OXPHOS complex I and IV defect, due to mutated complex I assembly factor C20ORF7, J. Inherit. Metab. Dis. 35 (2012) 125–131.
[32] M.R. Duchen, Contributions of mitochondria to animal physiology: from homeostatic sensor to calcium signalling and cell death, J. Physiol. 516 (1999) 1–17 (Pt 1).
[33] Y. Gong, M. Yi, J. Fediuk, P.P. Lizotte, S. Dakshinamurti, Hypoxic neonatal pulmonary arterial myocytes are sensitized to ROS-generated 8-isoprostane, Free Radic. Biol. Med. 48 (2010) 882–894.
[34] R. Paddenberg, B. Ishaq, A. Goldenberg, P. Faulhammer, F. Rose, N. Weissmann, R.C. Braun-Dullaeus, W. Kummer, Essential role of complex II of the respiratory chain in hypoxia-induced ROS generation in the pulmonary vasculature, Am. J. Physiol. Lung Cell. Mol. Physiol. 284 (2003) L710–L719.
[35] E.M. Redout, M.J. Wagner, M.J. Zuidwijk, C. Boer, R.J. Musters, C. van Hardeveld, W.J. Paulus, W.S. Simonides, . Right-ventricular failure is associated with increased mitochondrial complex II activity and production of reactive oxygen species, Cardiovasc. Res. 75 (2007) 770–781.
[36] S. Bonnet, G. Rochefort, G. Sutendra, S.L. Archer, A. Haromy, L. Webster, K. Hashimoto, S.N. Bonnet, E.D. Michelakis, The nuclear factor of activated T cells in pulmonary arterial hypertension can be therapeutically targeted, Proc. Natl. Acad. Sci. U.S.A. 104 (2007) 11418–11423.
[37] S. Bonnet, E.D. Michelakis, C.J. Porter, M.A. Andrade-Navarro, B. Thebaud, S. Bonnet, A. Haromy, G. Harry, R. Moudgil, M.S. McMurtry, E.K. Weir, S. L. Archer, An abnormal mitochondrial-hypoxia inducible factor-1alpha-Kv channel pathway disrupts oxygen sensing and triggers pulmonary arterial hypertension in fawn hooded rats: similarities to human pulmonary arterial hypertension, Circulation 113 (2006) 2630–2641.
[38] M.S. McMurtry, S. Bonnet, X. Wu, J.R. Dyck, A. Haromy, K. Hashimoto, E. D. Michelakis, Dichloroacetate prevents and reverses pulmonary hypertension by inducing pulmonary artery smooth muscle cell apoptosis, Circ. Res. 95

(2009) 830–840.
[39] S. Sharma, X. Sun, R. Rafikov, S. Kumar, Y. Hou, P.E. Oishi, S.A. Datar, G. Raff, J. R. Fineman, S.M. Black, PPAR-gamma regulates carnitine homeostasis and mitochondrial function in a lamb model of increased pulmonary blood flow, PLoS One 7 (2012) e41555.
[40] O. Warburg, F. Wind, E. Negelein, The metabolism of tumors in the body, J. Gen. Physiol. 8 (1927) 519–530.
[41] K. Chu, K.M. Boley, R. Moraes, S.H. Barsky, F.M. Robertson, The paradox of E-cadherin: role in response to hypoxia in the tumor microenvironment and regulation of energy metabolism, Oncotarget 4 (2013) 446–462.
[42] A. Chavez, L.F. Miranda, P. Pichiule, J.C. Chavez, Mitochondria and hypoxia-induced gene expression mediated by hypoxia-inducible factors, Ann. N. Y. Acad. Sci. 1147 (2008) 312–320.
[43] U.R. Jewell, M. Gassmann, Mammalian gene expression in hypoxic conditions, Zoology 104 (2001) 192–197.
[44] P.K. Majumder, P.G. Febbo, R. Bikoff, R. Berger, Q. Xue, L.M. McMahon, J. Manola, J. Brugarolas, T.J. McDonnell, T.R. Golub, M. Loda, H.A. Lane, W. R. Sellers, mTOR inhibition reverses Akt-dependent prostate intraepithelial neoplasia through regulation of apoptotic and HIF-1-dependent pathways, Nat. Med. 10 (2004) 594–601.
[45] A.J. Afolayan, A. Eis, R.J. Teng, I. Bakhutashvili, S. Kaul, J.M. Davis, G.G. Konduri, Decreases in manganese superoxide dismutase expression and activity contribute to oxidative stress in persistent pulmonary hypertension of the newborn, Am. J. Physiol. Lung Cell. Mol. Physiol. 303 (2012) L870–L879.
[46] S. Aggarwal, C.M. Gross, R. Rafikov, S. Kumar, J.R. Fineman, B. Ludewig, D. Jonigk, S.M. Black, Nitration of tyrosine 247 inhibits protein kinase G-1alpha activity by attenuating cyclic guanosine monophosphate binding, J. Biol. Chem. 289 (2014) 7948–7961.
[47] J.A. Cruz, E.M. Bauer, A.I. Rodriguez, A. Gangopadhyay, N.S. Zeineh, Y. Wang, S. Shiva, H.C. Champion, P.M. Bauer, Chronic hypoxia induces right heart failure in caveolin-1-/- mice, Am. J. Physiol. Heart Circ. Physiol. 302 (2012) H2518–H2527.
[48] S.A. Lorch, R. Foust 3rd, A. Gow, M. Arkovitz, A.L. Salzman, C. Szabo, B. Vayert, M. Geffard, H. Ischiropoulos, Immunohistochemical localization of protein 3-nitrotyrosine and S-nitrosocysteine in a murine model of inhaled nitric oxide therapy, Pediatr. Res. 47 (2000) 798–805.
[49] P. Oishi, A. Grobe, E. Benavidez, B. Ovadia, C. Harmon, G.A. Ross, K. Hendricks-Munoz, J. Xu, S.M. Black, J.R. Fineman, Inhaled nitric oxide induced NOS inhibition and rebound pulmonary hypertension: a role for superoxide and peroxynitrite in the intact lamb, Am. J. Physiol. Lung Cell. Mol. Physiol. 290 (2006) L359–L366.
[50] O. Rafikova, R. Rafikov, S. Kumar, S. Sharma, S. Aggarwal, F. Schneider, D. Jonigk, S.M. Black, S.P. Tofovic, Bosentan inhibits oxidative and nitrosative stress and rescues occlusive pulmonary hypertension, Free Radic. Biol. Med. 56 (2013) 28–43.
[51] Y.Y. Zhao, Y.D. Zhao, M.K. Mirza, J.H. Huang, H.H. Potula, S.M. Vogel, V. Brovkovych, J.X. Yuan, J. Wharton, A.B. Malik, Persistent eNOS activation secondary to caveolin-1 deficiency induces pulmonary hypertension in mice and humans through PKG nitration, J. Clin. Invest. 119 (2009) 2009–2018.
[52] H. Tang, J. Chen, D.R. Fraidenburg, S. Song, J.R. Sysol, A.R. Drennan, S. Offermanns, R.D. Ye, M.G. Bonini, R.D. Minshall, J.G. Garcia, R.F. Machado, A. Makino, J.X. Yuan, Deficiency of Akt1, but not Akt2, attenuates the development of pulmonary hypertension, Am. J. Physiol. Lung Cell. Mol. Physiol. 308 (2015) L208–L220.